Observations of Phytoplankton and Nutrients From a Lagrangian Drifter off Northern California

MARK R. ABBOTT,[1] KENNETH H. BRINK,[2] C. R. BOOTH,[3] DOLORS BLASCO,[4]
L. A. CODISPOTI,[5] PEARN P. NIILER,[6] AND STEVEN R. RAMP[7]

A Lagrangian drifter was deployed in a cold filament off northern California as part of the Coastal Transition Zone program. The drifter was equipped with an optical package (consisting of a spectroradiometer, a fluorometer, and a beam transmissometer) suspended at 8.5–m depth and a water sampler suspended at 16.3–m depth. The drifter was recovered after 8 days. Optical, chemical, and biological properties changed considerably as the drifter moved offshore in the cold filament. Concentrations of phytoplankton chlorophyll increased rapidly in the first 2 days, in parallel with the disappearance of nitrate and nitrite. After this initial period, chlorophyll decreased gradually over the next 6 days with prominent diurnal fluctuations present in the last 3 days. Water transparency also showed similar long-term as well as diurnal fluctuations. The phytoplankton community became increasingly dominated by large centric diatoms throughout the deployment. Although total cell volume was higher towards the middle of the deployment, this increase occurred without a parallel increase in chlorophyll. In addition, total particulate concentrations were highest nearshore. Although the drifter slippage was approximately 1 cm/s, the biological, chemical, and physical characteristics of the water were affected by both in situ changes and vertical motions of the water. These results are generally consistent with results from other upwelling studies.

1. INTRODUCTION

Unattended observations of biological and optical properties of the upper ocean are relatively new in oceanographic research [e.g., *Dickey*, 1988]. Recent studies have been reported using fluorometers [*Whitledge and Wirick*, 1983; *Fukuchi et al.*, 1988; *Walsh et al.*, 1988] and spectroradiometers [*Dickey et al.*, 1986]. Such moorings will provide high-resolution time series data on biological processes that should greatly improve our understanding of the dynamics of the upper ocean. In this paper we present results from a Lagrangian drifter that was equipped with a spectroradiometer, a fluorometer, a transmissometer, and an automated water sampler as part of the Coastal Transition Zone (CTZ) program off northern California in 1987 [*Coastal Transition Zone Group*, 1988].

The large filaments observed off the west coast of the United States have been noted in satellite imagery for several years [*Breaker and Gilliland*, 1981; *Traganza et al.*, 1983; *Coastal Transition Zone Group*, 1988]. They can extend seaward several hundred kilometers and are often characterized by high water velocities [*Kosro and Huyer*, 1986; *Kosro*, 1987; *Flament et al.*, 1985]. Several mechanisms have been proposed for the formation and maintenance of the filaments including baroclinic instabilities [*Ikeda and Emery*, 1984; *Willmott*, 1984], interaction between wind forcing and coastal topography [*Kelly*, 1985], alongshore

---
[1]College of Oceanography, Oregon State University, Corvallis.
[2]Woods Hole Oceanographic Institution, Woods Hole, Massachusetts.
[3]Biospherical Instruments, Incorporated, San Diego, California.
[4]Bigelow Laboratory for Ocean Sciences, West Boothbay Harbor, Maine.
[5]Monterey Bay Aquarium Research Institute, Pacific Grove, California.
[6]Scripps Institution of Oceanography, University of California, San Diego, La Jolla.
[7]Department of Oceanography, U.S. Naval Postgraduate School, Monterey, California.

pressure gradients [*Davis*, 1985a,], and offshore eddies [*Mooers and Robinson*, 1984].

Because these filaments are relatively persistent when compared with phytoplankton time scales, it has been proposed that they may be especially important to the primary production of the California Current system. Estimates of the transport (of the order of 2 Sv [*Kosro and Huyer*, 1986]) when coupled with the higher than average nutrient concentration nearshore suggest that they may also be important in the overall nutrient balance. It has been suggested that the filament may be a relatively isolated feature with relatively little exchange between itself and surrounding waters. Such isolation would result in distinct changes in the biological properties of the filament as the water moves offshore and "ages." By making Lagrangian observations of biological and chemical properties, we hoped to estimate the time scales of these changes as well as assess the relative roles of in situ processes versus exchange processes in creating these changes.

Our results support the general view of upwelling ecosystems that has been developed over the last 2 decades. That is, freshly upwelled water is characterized by high nutrients, low phytoplankton biomass, and cold temperatures. As this water advects away from the upwelling center, it warms, phytoplankton take up nutrients, and biomass increases. As phytoplankton continue to grow, nutrients become depleted. Phytoplankton growth is greatly reduced, eventually resulting in a decrease in phytoplankton biomass as losses due to sinking or grazing dominate. These four stages correspond to the zones proposed by *Jones et al.* [1983] and described by *MacIsaac et al.* [1985] for the Peru upwelling system. We describe a number of processes that occur on small time and space scales within this larger framework. We will compare the observed biological variability with the physical environment and discuss how the biological response to the filament changes over time.

2. INSTRUMENTATION AND METHODS

Lagrangian drifters have been used successfully in recent years in studies of surface layer currents [*Davis*, 1985a, b; *Niiler et al.*, 1988; *Poulain et al.*, 1987]. The possibility of attaching instrumentation to such drifters is appealing, as it will help reduce the

co-mingling of temporal and spatial variability. There have been numerous studies where biological sampling has been guided by drifter tracks [Ryther et al., 1971; Scripps Institution of Oceanography, 1974; MacIsaac et al., 1985; Mackas et al., 1989]. Although not all of these studies used Lagrangian drifters, the basic goal of the studies was to separate advective effects (Eulerian) from in situ (Lagrangian) effects. Such a separation would allow the study of temporal variability without being concerned with spatial variability that may be confused with temporal variability through the process of advection. However, distinguishing between spatial and temporal variability is not a simple task with Lagrangian drifters that are fixed at one depth, since vertical movement of water (and biological materials) may be significant.

During the first field year of the CTZ program [Coastal Transition Zone Group, 1988], we deployed an optical package, a water sampler, and a thermistor chain on a TriStar-II drifter [Niiler et al., 1988]. The TriStar-II telemeters its position, along with surface temperature, via the Argos satellite tracking system. The uninstrumented drifter configuration is known to move with the ambient flow to within about 1 cm/s. Figure 1 is a schematic of the instrumented drifter. The optical package was mounted approximately 4.5 m above the drogue center at a depth of about 8.5 m. The package consisted of a Biospherical Instruments MER-2020 spectroradiometer [Booth and Smith, 1988], a SeaTech 25-cm beam transmissometer, and a SeaTech strobe fluorometer. The spectroradiometer measured both upwelling radiance and downwelling irradiance at five wavelengths, instrument attitude, temperature, depth, and housekeeping information which were recorded on an internal data acquisition system. There was an additional upwelling radiance measurement made at 683 nm by a detector optimized to respond to sun-stimulated fluorescence by chlorophyll. This system also recorded the transmissometer and fluorometer data. The instruments were turned on for 45 s every 4 min, and the average for the last 30 s was stored. This allowed the fluorometer and transmissometer to warm up and stabilize. Table 1 gives a complete list of the data recorded on the data acquisition system. The automated water sampler [Friederich et al., 1986] was mounted directly below the drogue at a depth of 17.5 m and was programmed to sample the water at twenty 6-hour intervals. At each sampling time, two 20-cm^3 syringes, one filtered and one not, drew in water samples for nutrient and phytoplankton counts, respectively. Both water samples were preserved in situ. Lugol's solution was used to preserve the phytoplankton samples, and the nutrient samples were preserved with mercuric chloride and analyzed as described by Friederich et al. [1986]. Finally, a 50-m recording thermistor chain was hung directly below the water sampler, but it did not return enough good data to be useful.
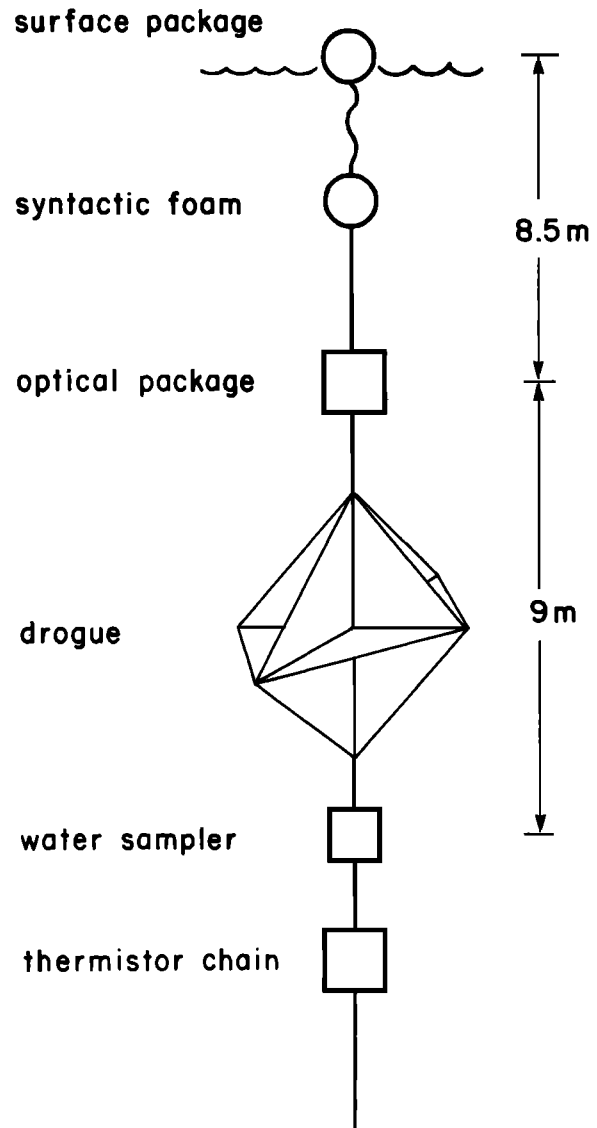

Fig. 1. Schematic of Tri-Star II drifter with water sampler, thermistor chain, and optical package.

3. Results

Drifter Trajectory and Relationship with Hydrographic Structure

The instrumented drifter was launched on June 17, 1987 (Julian day 168) at 1112 LT and recovered on June 25 (Julian day 176) at

TABLE 1. Variables Recorded on Biospherical Instruments MER-2020 Spectroradiometer

Variable	Description
Downwelling Irradiance, nm	410, 441, 488, 520, 560
Upwelling Radiance, nm	410, 441, 488, 520, 683
Other variables	strobe and sun-stimulated fluorescence, beam transmission, temperature, depth
Housekeeping variables	time, tilt angle (2), ground voltage, battery voltage

1235 LT. Its deployment location was chosen to be at the center of the nearshore end of a pronounced cold filament detected by hydrographic surveys off Point Arena, California, and by remote sensing (Figure 2). The drifter track show in Figure 2 is a spline fit to the actual locations provided by the Argos II system roughly eight times per day. Figure 3 is the drifter speed estimated from the drifter displacements, using the smoothed location data. Note that the drifter moved slowly on days 170–172 and rapidly on days 173–175. The drifter stayed in the core of the cold, dense feature for as long as the track could be meaningfully compared with the hydrographic survey which was completed on day 170. During the same time interval (days 168–170), the drifter tended roughly to follow contours of constant 10/500 dbar dynamic height (Figure 4). The extra instrumentation (and hence drag) on this particular drifter did not seem to affect its water-following characteristics; other drifters deployed at the same time behaved similarly. A detailed comparison of the instrumented drifter with four other drifters surrounding it showed that the instrumented drifter moved about 10% more slowly than the others along the filament. This is not surprising, as 50 m of thermistor cable provides a substantial connection between the shallow drogue and the slower moving, deep water. Figure 5a is the alongshore component of the wind stress measured by National Data Buoy Center (NDBC) buoy 46013 (38°13'N, 123°18'W). The wind vectors have been rotated 47° so that the alongshore component is roughly parallel to the coast. The tendency to follow dynamic height contours, of course,
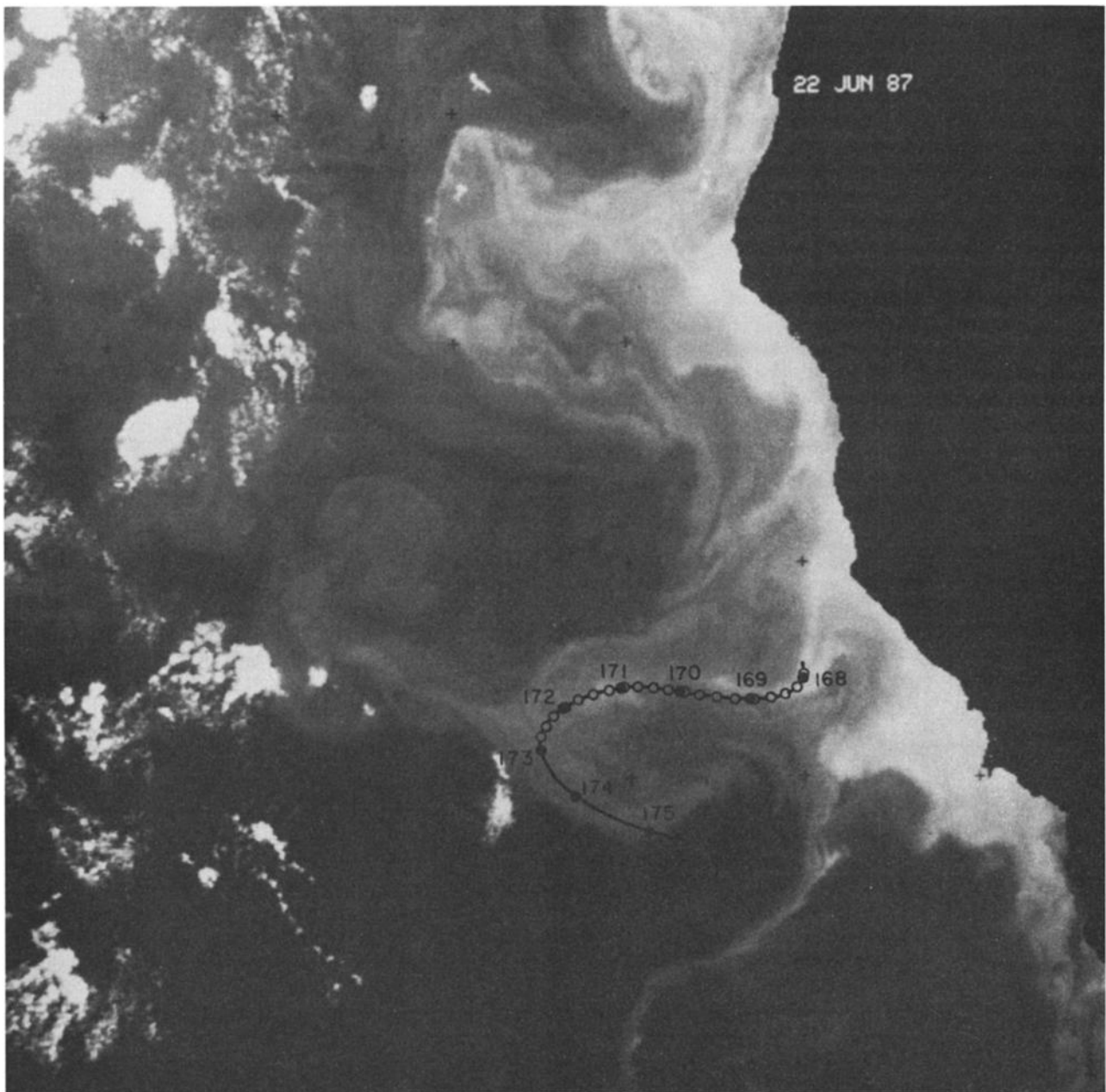

Fig. 2. Overlay of smoothed drifter track on AVHRR image of sea surface temperature acquired on June 22,1987. Cooler temperatures are lighter shades. Open circles on drifter track represent water sample locations. Solid circles represent location of drifter at 1700 LT on each day of the deployment.
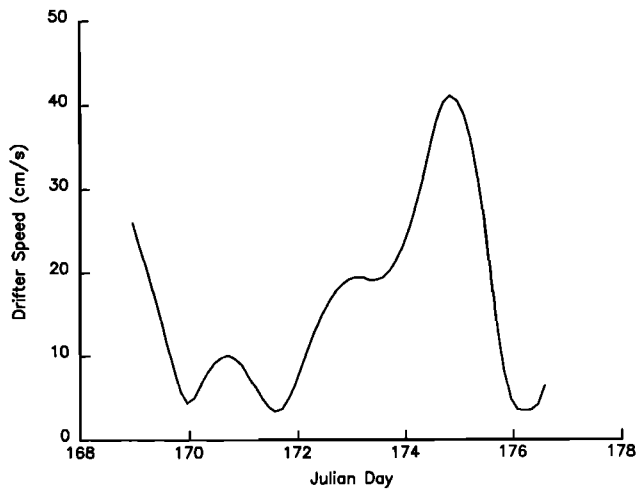
Fig. 3. Drifter speed as estimated from displacements along smoothed drifter track.

suggests a substantial geostrophically balanced flow component. To the extent that the drifter does not follow the dynamic height contours, errors in reference level of the geostrophic calculation or the presence of ageostrophic velocity components can be credited. Also, the geostrophic contours may not be well resolved in this area. The most likely ageostrophic effect is Ekman transport within the surface boundary layer.

During the initial 18 hours of the deployment, the apparent deviation from geostrophy was particularly evident, since the drifter went roughly perpendicular to the local dynamic height contour (Figure 4). At the same time, the winds were relatively strong (8.5 m/s) towards the southwest (Figure 5a). This converts
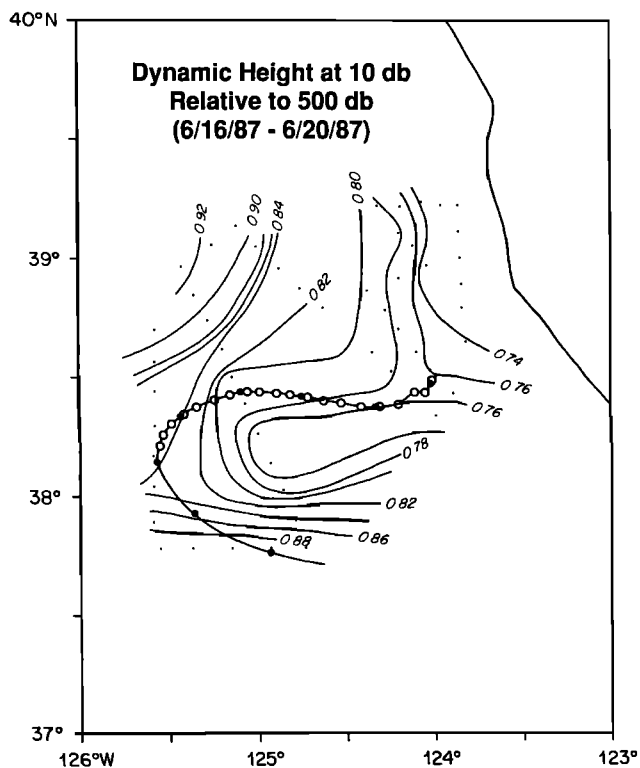

Fig. 4. Dynamic height from hydrographic survey of June 18–24, 1987, with drifter track overlain.

to a surface wind stress of about 1.0 dyn/cm^2 towards 123.5°T or a surface Ekman transport of 1.1 m^3/s toward 213°T. If we assume a slablike mixed layer of 10– to 20–m thickness, this would yield a southwestward ageostrophic displacement of 4–7 km. The observed displacement of the drifter was 14 km in the proper direction. Thus Ekman drift is not adequate to account for the offset of the drifter, although it is clearly large enough to be an important influence. Other factors, such as incorrect reference level for the geostrophic calculations or other ageostrophic forces besides wind drift, may be important during this period.

Both the drifter temperature records (Figure 5b) and the drifter track relative to the near-surface temperature field (Figure 2) suggest that the water warmed as the drifter moved offshore. This warming may be attributable to the drifter's movement offshore through the general cross-shore temperature gradient (warmer water tends to be offshore), but at least some of the temperature behavior seems to be related to the local winds. Specifically, much of the warming took place during days 170–172 when the winds were relatively weak (Figure 5a) and the mixed layer was presumably warming and stabilizing due to surface heating. This stabilization is indicated by a tendency for the sea surface temperature (SST) (indicated by the crosses in Figure 5b) to be warmer than the 8.5–m temperature by as much as 0.5°C. During this presumably stable period, the 8.5–m temperature series shows considerable high-frequency (1– to 6–hour period) variability which is likely to be associated with internal wave activity in a now stratified upper ocean. However, the temperature increase of 2.5°C in 2.5 days would imply a net heating rate of the 25–m-deep mixed layer by 1210 W/m^2. Since only 10% of this upper ocean temperature change can be attributed to the net heating, this temperature increase must therefore be due to the convergence of warm water at 8 m, a net downwelling, or the drifter's moving into warmer water. As the latter effect is not apparent in the advanced very high resolution radiometer (AVHRR) image (Figure 2), we conclude that the 11°C water sank to deeper depths below the drifter and warmer water replaced it on the surface. On day 171 the winds increased, leading to a relative homogenization of upper ocean temperatures, consistent with the similarity of the two temperature records during the last 4 days of the deployment. Diurnal cycles of temperature are also evident during this last period along with a slight cooling trend. The steplike changes in temperature during days 169–170 (typically 0.4°) may be the result of the drifter's crossing frontal or interleaving regions.

Optical Data

Figures 6a, 6b, 6c, and 6d show downwelling irradiance at 520 nm, beam attenuation, strobe fluorescence, and upwelling radiance at 683 nm. There was considerable variability in the daily amount of downward irradiance (Figure 6a). Days 169, 170, and 171 (June 19, 20, and 21) were relatively cloudy, with higher-frequency variations associated with passing clouds. Note that on days 172 and 173, winds were high (Figure 5a) and skies were clear. This is the usual condition during the upwelling season off northern California [e.g., *Abbott and Zion*, 1987; *Simon*, 1977], where strong equatorward winds are associated with a shallowing of the marine boundary layer which is unfavorable for the formation of low stratus clouds. As the winds relaxed on days 174 and 175, cloudiness increased. Note that we choose to present downwelling irradiance at 520 nm as an indicator of solar radiation, as *Gordon et al.* [1988] have shown that irradiance at 520 nm is relatively invariant with changes in phytoplankton pigment con-
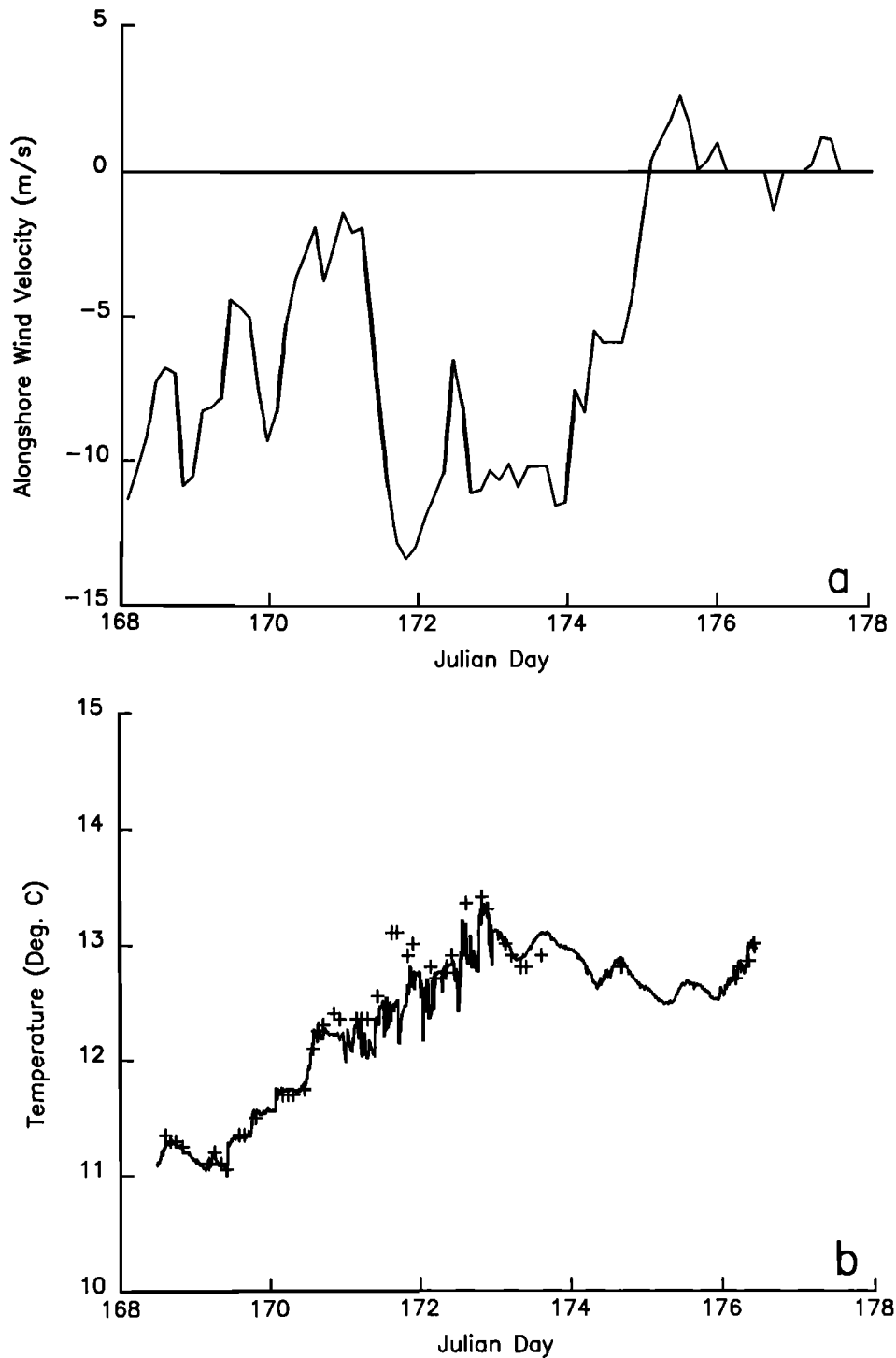
Fig. 5 (a) Alongshore component of wind velocity from NDBC buoy 46013. Winds were rotated 47° to be parallel to coast. (b) Temperature along drifter track from thermistor mounted in optical package (8.5 m depth). Crosses represent measurements from the thermistor mounted in surface transmitter package.

centration. Although no special precautions were taken to prevent fouling of the optical instruments, visual inspection and cleaning after recovery revealed no signs of fouling. Note that beam attenuation (Figure 6b) decreased through the period, suggesting that fouling was not significant.

The beam attenuation coefficient (Figure 6b) was calculated using the formulas of *Bartz et al.* [1978]. There appear to be several time scales of variability. First, there is a long-term in-

crease in water clarity, consistent with a decrease in suspended particulate concentration. Second, there is a diurnal cycle which is particularly apparent near the end of the deployment. Figure 7 shows the transmission data from the last 3 days of the deployment in greater detail. Note that the attenuation is lowest just before sunrise, increases steadily through the day, reaches a maximum at sunset, and then begins to decrease again. This is consistent with results from the central Pacific reported by *Siegel*
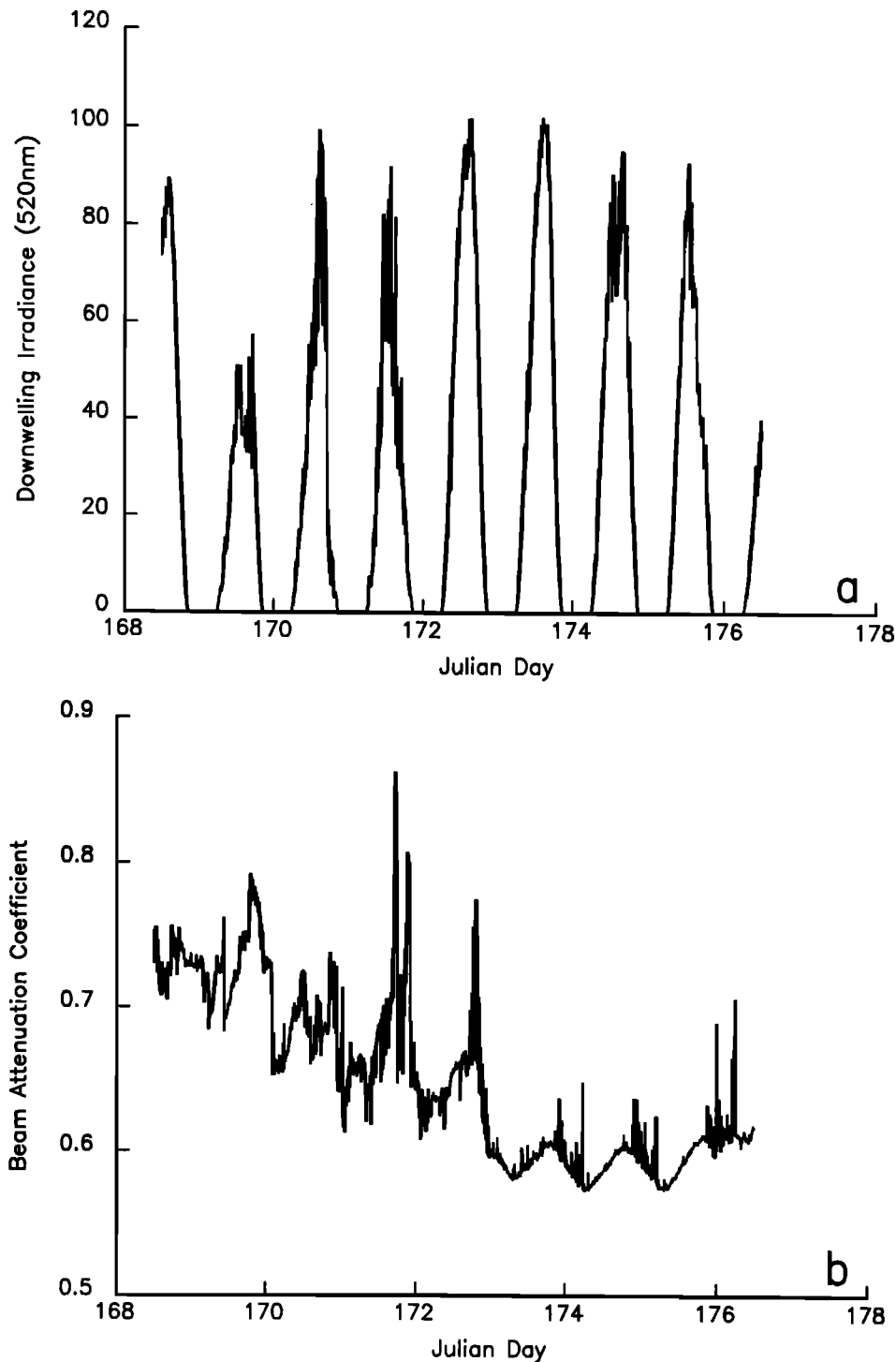
Fig. 6. (a) Downwelling irradiance (μW cm^{-2} nm^{-1}) at 520 nm. (b) Beam attenuation coefficient (m^{-1}) at 660 nm from 25-cm beam transmissometer. (c) Strobe-stimulated fluorescence (volts). (d) Upwelling radiance (μW cm^{-2} nm^{-1} str^{-1}) at 683 nm (sun-stimulated fluorescence).

et al. [1989], who propose that these changes are largely the result of phytoplankton growth during the day and subsequent grazing at night by zooplankton. Note that in this case, the accumulation of particles during the day is nearly balanced by losses (presumably grazing and sinking) at night during the last days of the deployment. The third time scale is a series of sharp decreases in transparency that occur primarily on days 174, 175, and 176. If we look in detail at the last 3 days of the deployment in Fig-

ure 7, we see that these large decreases occur primarily between sunset and midnight. Figures 8a and 8b show the relationship between strobe fluorescence and beam attenuation for the nighttime data only. Note that the changes in attenuation are highly correlated with changes in fluorescence on the first two nights. This correlation breaks down on subsequent nights. (A similar lack of correlation was present for the remainder of the deployment.) This is consistent with vertical migration of microzooplankton through
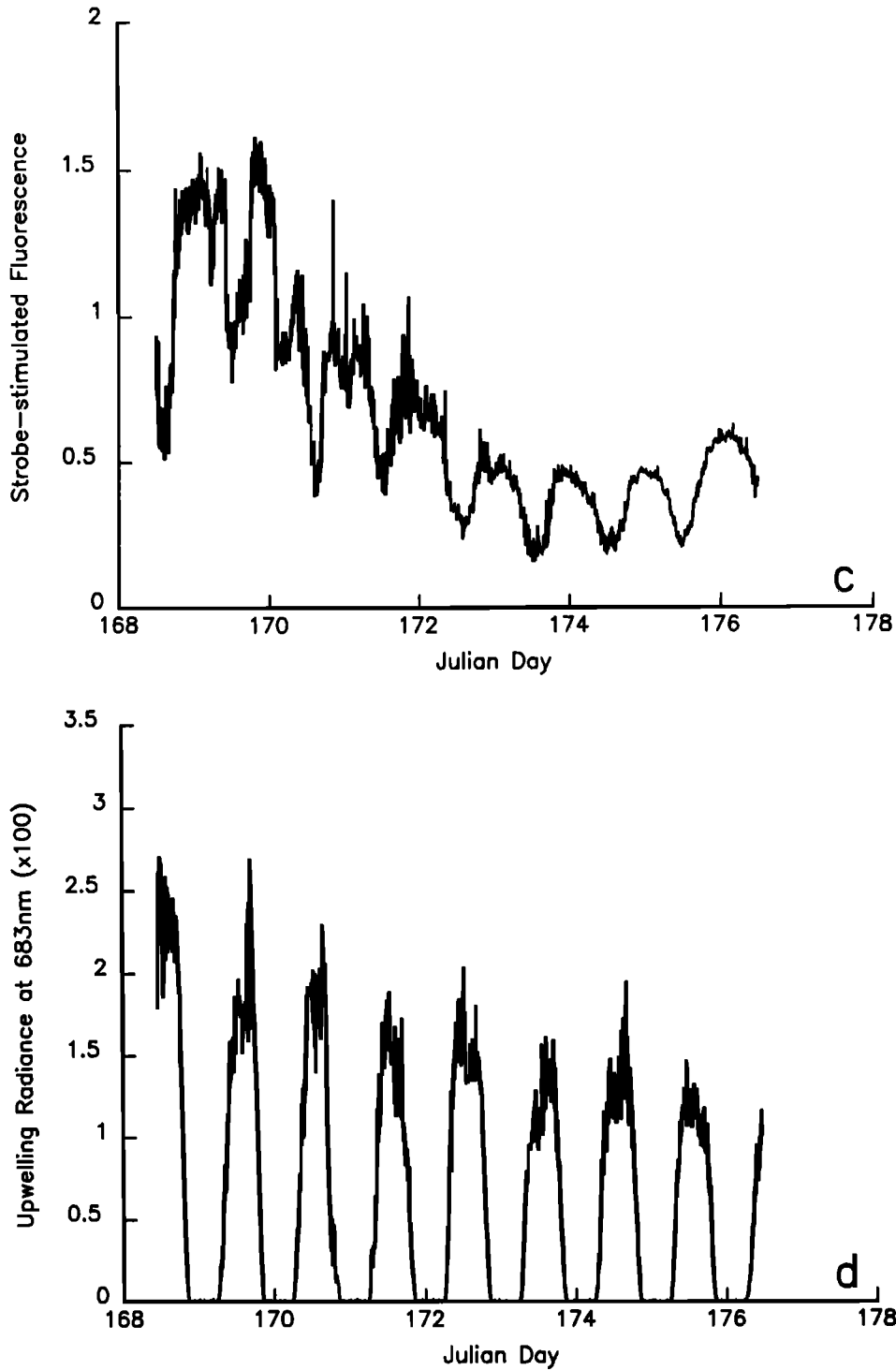
Fig. 6. (continued)

the beam transmissometer at nighttime during the latter part of the deployment. In the first days of the deployment, changes in attenuation are largely the result of changes in concentration of fluorescent particles, presumably phytoplankton.

Strobe-stimulated fluorescence (Figure 6c) shows a strong diurnal signal which arises from both physiological changes in the phytoplankton [Kiefer, 1973; Harris, 1980] and changes in chlorophyll abundance. Fluorescence responds to changes in nutrient status, light history, species composition, and a variety of other factors [Kiefer, 1973; Abbott et al., 1982]. Unfortunately, we

do not have an independent estimate of chlorophyll for each day (this would be possible if the upwelling radiance signals had not been contaminated by the drogue). However, fluorescence declines by roughly a factor of 3 over the term of the deployment, with the bulk of the decrease occurring in the first 4 days. These changes were highly correlated with changes in beam attenuation (r^2=0.65) over the whole data record. Thus it appears that the strobe-stimulated fluorescence measurement is a reasonable indicator of phytoplankton pigment concentration if we account for the diurnal changes in fluorescence response.
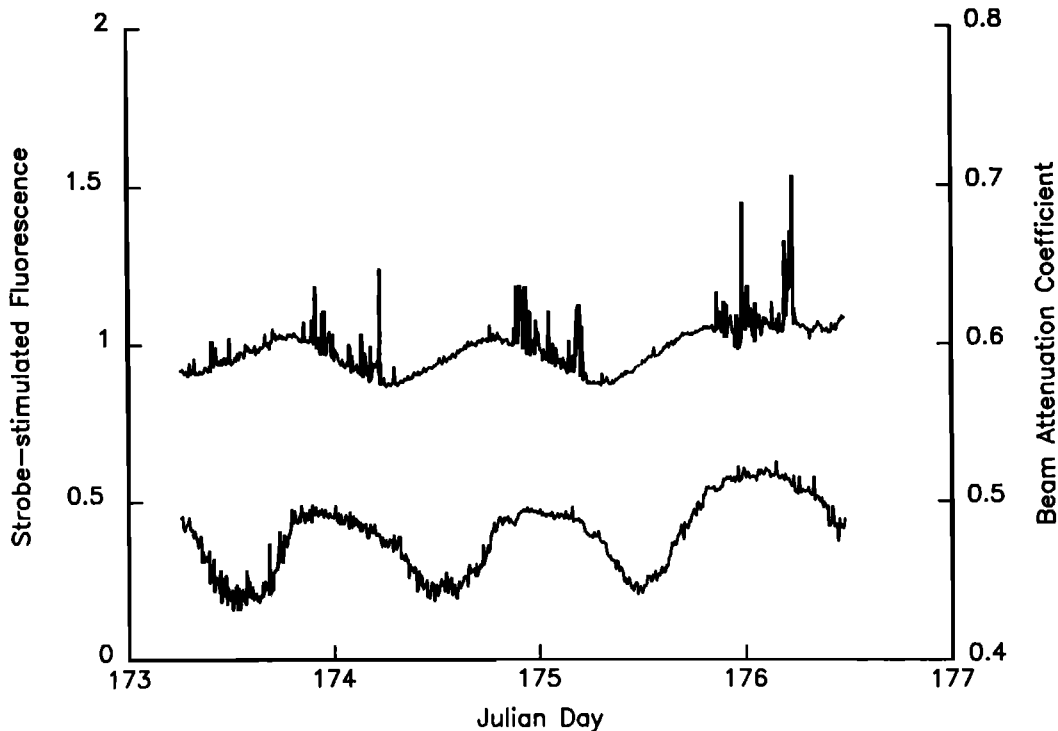
Fig. 7. Beam attenuation (upper line) and strobe-stimulated fluorescence (lower line) from last 3 days of drifter deployment.

The regression of beam attenuation on strobe-stimulated fluorescence yielded a slope of 0.131 $(m\ V)^{-1}$ and an intercept of 0.564 m^{-1}. If we assume that beam attenuation is the sum of the attenuation due to water, fluorescent particles, and nonfluorescent particles, then the intercept should represent the attenuation due to water and nonfluorescent particles. Since the expected range of the beam attenuation coefficient at 660 nm for pure water ranges between 0.31 and 0.42 m^{-1} [Tyler et al., 1974], this suggests that there was a large component of nonfluorescent material in the water. As zooplankton may significantly affect beam attenuation and they appear mainly at night, we recalculated the regression for daytime data only. However, the slope and intercept were essentially unchanged. We then examined the period from day 168 through day 172 separately from the period covering day 173 through day 176. For the early period, the slope was 0.076 m^{-1} and the intercept was 0.627 $(m\ V)^{-1}$. For the late period, the slope was 0.078 $^{-1}$ and the intercept was 0.564 $(m\ V)^{-1}$. The decrease in the intercept over time suggests that there is a decrease in the amount of nonfluorescent particulate material in the water as the drifter moves along its path.

Except for the 683-nm wavelength, we suspect that the other upwelling radiance channels may have been contaminated by the presence of the large, multicolored drogue underneath the instrument. The 683-nm upwelling radiance bands were likely to be uncontaminated because of the strong absorption of light in this portion of the spectrum. Thus radiance detected at this wavelength would originate near the detector [Kiefer et al., 1989]. Figure 6d (683-nm upwelling radiance) is a measure of sun-stimulated fluorescence. As described by Booth et al. [1987], this fluorescence may be an indicator of the photosynthetic potential of the phytoplankton. Figures 9a and 9b show the variation of strobe-stimulated fluorescence versus downwelling irradiance at 520 nm. Note the strong decrease in the slope of these curves beginning on the third day of the deployment. Chlorophyll (as measured through extractions from samples collected at the drifter release

and recovery points) decreased during this period from about 1 mg/m^3 to 0.2 mg/m^3 (C. Davis, personal communication, 1987). The magnitude of this decrease is consistent with the decrease in the daily maximum of strobe-stimulated fluorescence observed over this period.

Water Sampler Data

Nitrate + nitrite (N+N) concentrations as measured by the drifter's water sampler are shown in Figure 10. Initially, N+N concentrations are high (>10 μM), which taken with the low surface temperatures (Figure 5b) suggest that the drifter was deployed in freshly upwelled water. It would then be expected that the N+N concentration would decrease monotonically as it is taken up by phytoplankton. This smooth decrease was observed only during the first 2 days of deployment. After the start of day 170, the N+N concentration varied considerably over the next 2 days, as the drifter appeared to move through an area of discrete temperature fronts (Figure 5b). Most likely, the changes in N+N were a result of changes in water masses, rather than being a result of purely biological processes. These abrupt changes in water types suggest that the drifter did not follow water parcels exactly. Alternatively, the sampler could have been in a nitracline which was moving as a result of vertical motions. As winds were relatively light and the upper layer of the ocean was stratified (Figures 5a and 5b), vertical motions could appear as horizontal variability. After day 172 the drifter remained in waters with low N+N concentrations.

The N+N time series gives the impression that the drifter experienced at least three distinct regimes. Figure 11 shows the relationship between temperature and N+N during the deployment. Note that initially the drifter was in a region of low temperatures and high N+N. Later, the drifter passed through a region of more variable temperature and N+N with generally higher temperature and lower N+N. Finally, the drifter entered an area of high temperature and barely detectable N+N.
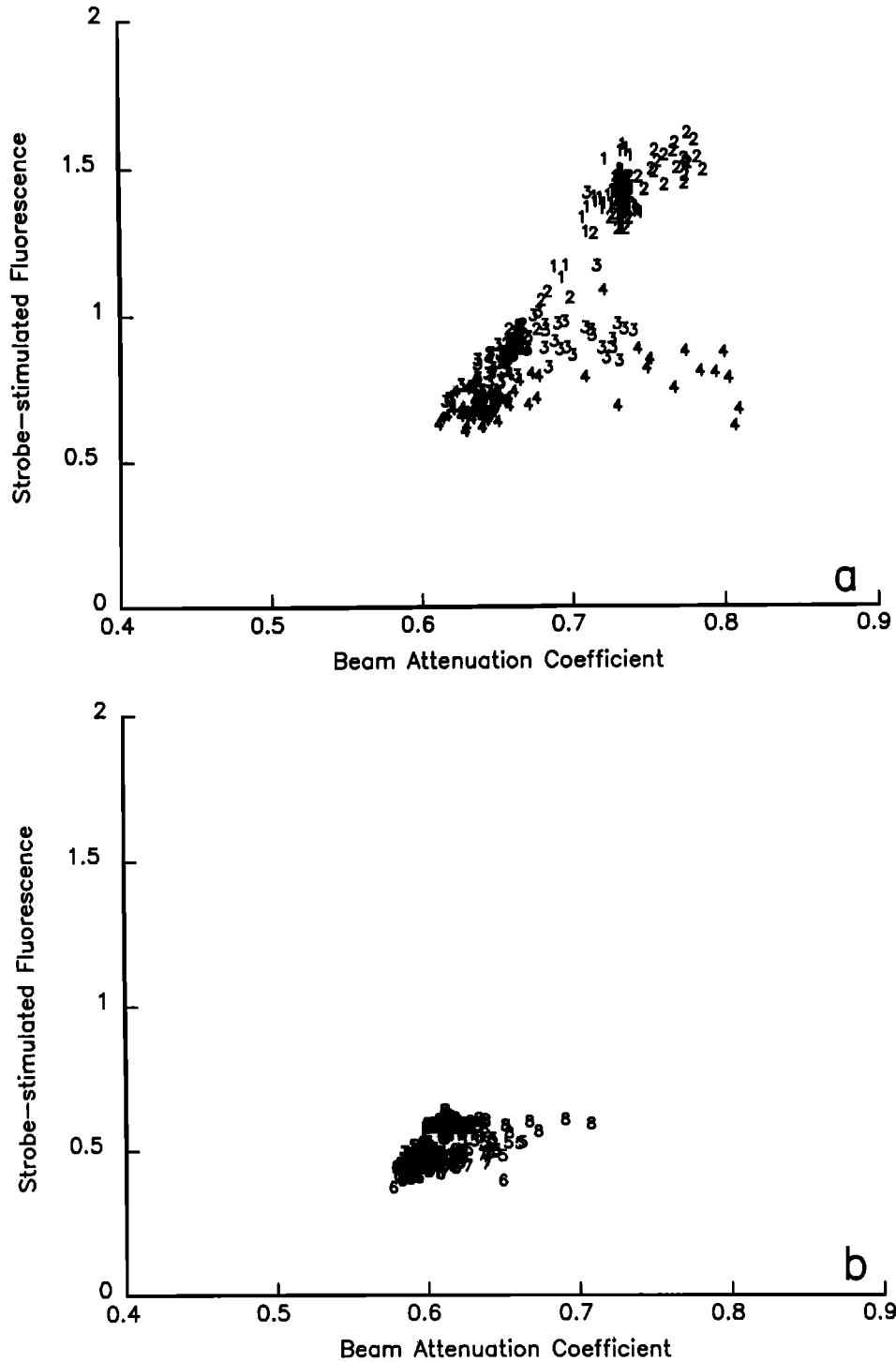
Fig. 8. (a) Strobe-stimulated fluorescence versus beam attenuation for nighttime data only for the first 4 days of the drifter deployment. Numbers correspond to the day of deployment. (b) As in Figure 8a except for days 5–8 of the deployment.

We can estimate primary productivity based on the disappearance of N+N during the initial two days of deployment. Approximately 10 μM of nitrate was taken up in 2 days. If we assume a C:N ratio of 106:16 based on the Redfield ratio, then the uptake of nitrate corresponds to a carbon uptake rate of about 465 mg C/m^3/day. This value is comparable to that for the Peru upwelling [Brink et al., 1981; Ryther et al., 1971] and is within the range of values reported for CalCOFI stations in this region [e.g., Scripps Institution of Oceanography, 1984]. However, this is probably an overestimate, as some of the disappearance of nitrate was likely

the result of physical mixing processes, in addition to biological uptake. The considerable variability (and reappearance) of N+N suggest that water mass changes as well as biological uptake are likely to be important. However, phytoplankton cell volume (Figure 10) and chlorophyll (as indicated by strobe-stimulated fluorescence in Figure 6c) both doubled during the first 2 days of the deployment.

Figure 10 also includes the total cell volume based on phytoplankton counts, using an average cell volume calculated for each taxonomic group that was counted. Note that cell volume
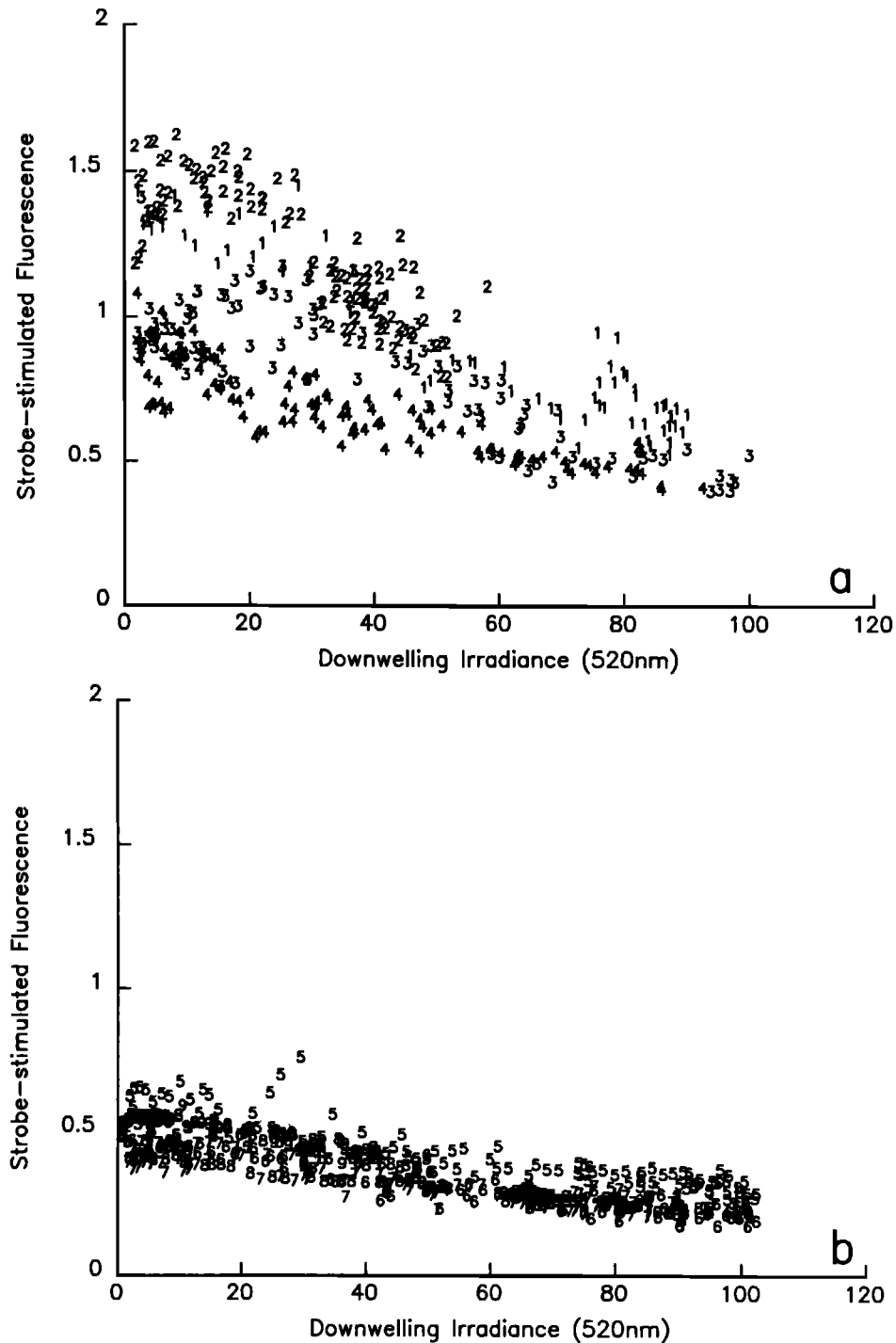
Fig. 9. (a) Strobe-stimulated fluorescence versus downwelling irradiance at 520nm for the first 4 days of the deployment. Numbers correspond to the day of the deployment. (b) As in Figure 9a except for days 5–8 of the deployment.

increased by nearly 2 orders of magnitude between days 168 and 173, although there is considerable variability between days. Some of these changes may result from travel through different water masses by the drifter, rather than just in situ changes. Note the significant decrease in total volume in the last sample on day 173.

The composition of the phytoplankton community is shown in Figure 12 as a percentage of total cell volume. *Chaetocerus* and large, centric diatoms dominate the community from the beginning until day 170. After this point, the large centric diatoms

dominated the community. Although the centric diatoms in our samples were identified as a mixture between *Actinocyclus* and *Thalassiosira* spp., it is difficult to distinguish between these two groups without using electron microscopy. *Hood et al.* [1990] collected a sample from this region a few days before the drifter deployment. Their (in collaboration with E. Venrick) scanning electron micrograph results showed that the centric diatoms were largely *Actinocyclus*. Note that changes in the dominance of these large centric diatoms (hereinafter referred to as LCD) are largely correlated with changes in total cell volume. There appear to
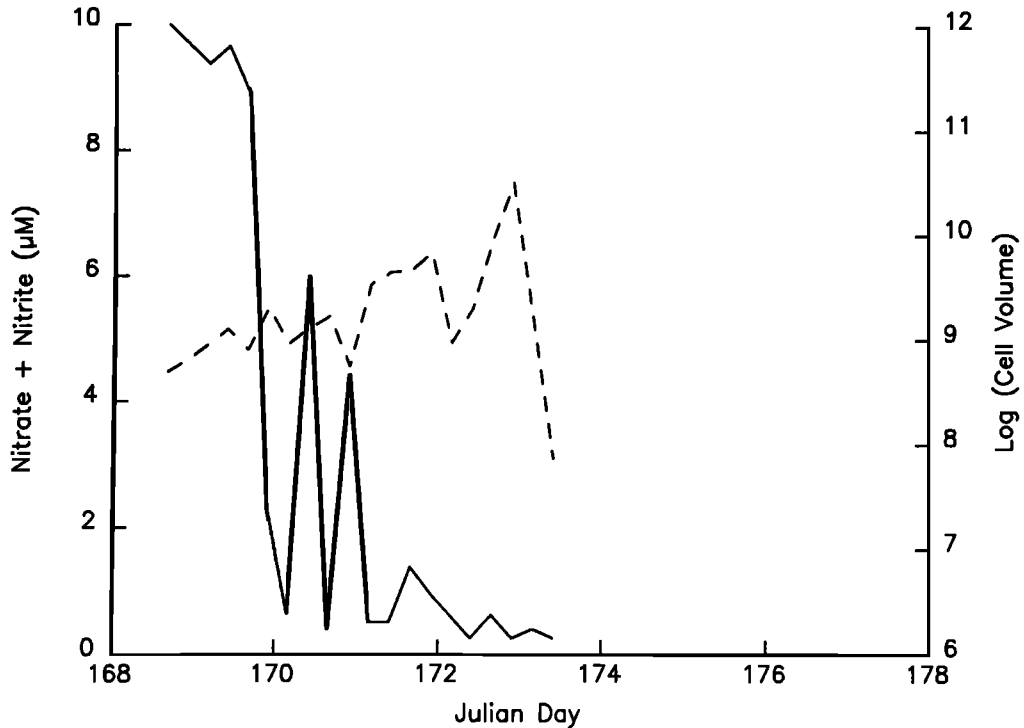
Fig. 10. Nitrate + nitrite (N+N) concentrations (solid line) and logarithm of total phytoplankton cell volume in $\mu m^3/10$ m*l* (dashed line) during the deployment.

have been three distinct phytoplankton assemblages. The first was a nearshore community, consisting primarily of *Chaetocerus* and LCD. The total cell volume was fairly low in this region. The diatom community in the second regime (beginning late on day 169 and extending through day 171) was primarily *Rhizosolenia* and *Nitzschia* with a decreasing percentage of *Chaetocerus* and an increasing percentage of LCD. The third assemblage was

largely LCD. Note that these periods corresponded fairly well to the delineations based on temperature and N+N concentration described earlier.

4. DISCUSSION

As the slippage characteristics of the drifter are of the order of 1 cm/s, we expect that the drifter may be as much as 10 km away
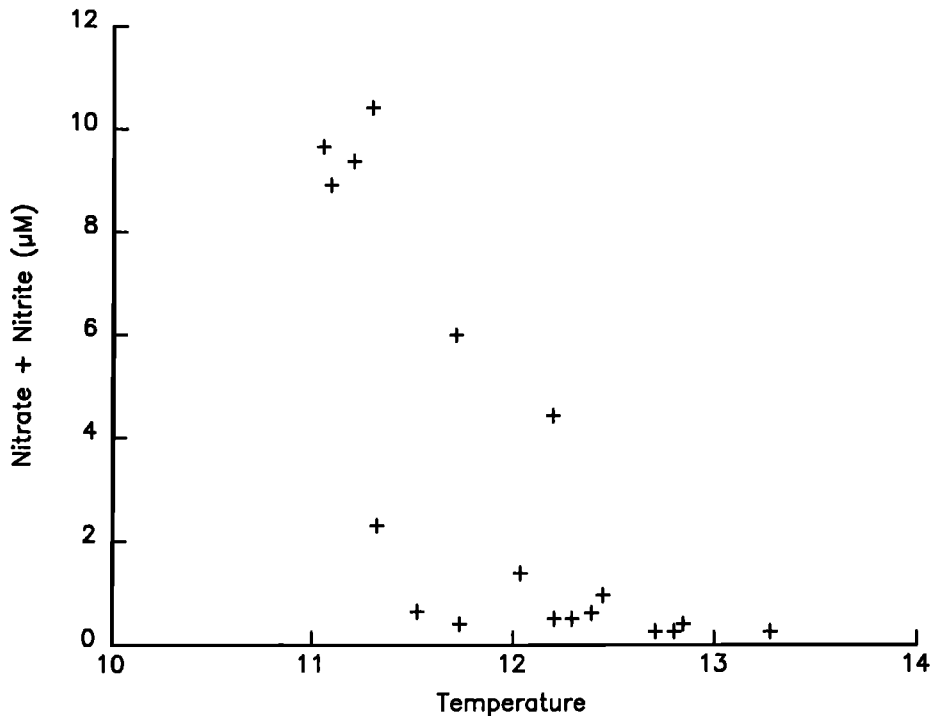

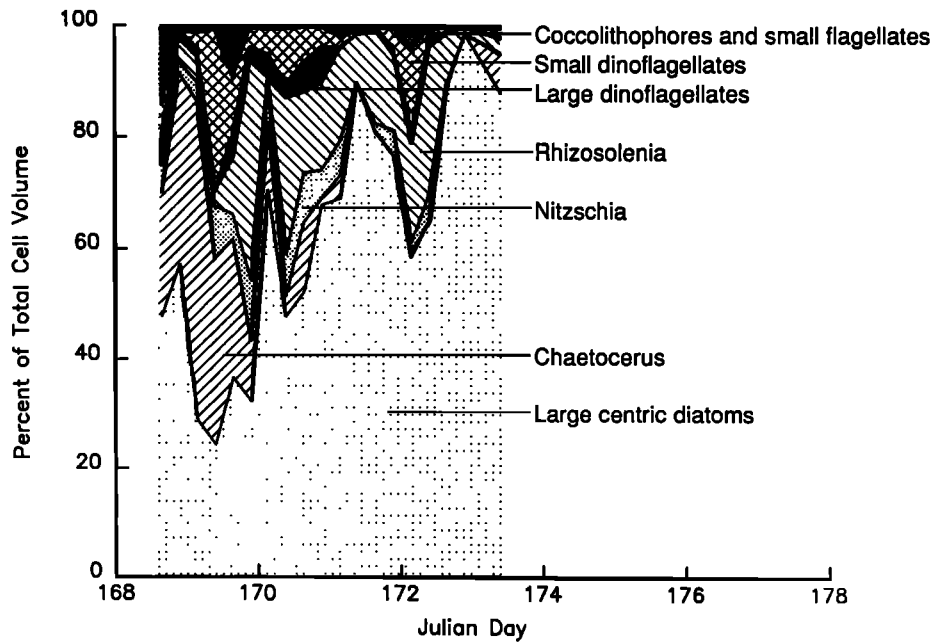Fig. 11. N+N concentrations versus temperature at 8.5 m.

Fig. 12. Percent of total cell volume for the major phytoplankton groups.

from the original water mass by the end of the deployment. This could be a considerable deviation in regions such as the filament, where horizontal gradients are large. Further, the possibility of changes in water properties through mixing, exchange with surrounding water, or through subduction of the water mass, may complicate matters. Although the Tristar-II has excellent horizontal water-following properties, it is constrained to a fixed depth so, strictly speaking, it is only a quasi-Lagrangian drifter. Thus the temporal changes that we observed were some complicated function of slippage, in situ changes, and changes in water mass characteristics resulting from mixing and vertical motions of the water. However, the drifter track itself appears to follow the strong temperature signature of the filament present at the water surface (Figure 2), suggesting that the large-scale changes may be due to in situ processes.

Using all of these data sets, we can identify three distinct regimes or types on the basis of their physical/chemical characteristics as well as on their biological properties. The first type was located nearshore and is characterized by low temperatures, high N+N, low light transmission, high strobe-stimulated fluorescence and sun-stimulated fluorescence, low total phytoplankton cell volumes and high relative proportions of LCD and Chaetocerus. On the basis of the hydrographic survey, this type is located near the origin of the cold, seaward-moving filament. Although this apparently freshly upwelled water had all of the characteristics typical of such conditions noted in upwelling regions [e.g., Beers et al., 1971; Jones et al., 1983; Brink et al., 1981; Abbott and Zion, 1985], note that beam attenuation (Figure 6b) is high despite the relatively low total cell volume (Figure 10) but consistent with the high strobe-stimulated fluorescence values (Figure 6c). We suspect that this water also contained significant amounts of detritus and other suspended material as has been seen in freshly upwelled water off Point Conception [Jones et al., 1983]. However, changes in water transparency were generally well correlated with changes in strobe-stimulated fluorescence, indicating that this material may have been of phytoplankton origin as long as we can assume that strobe-stimulated fluorescence is a reasonable indicator of phytoplankton biomass (Figure 6c). At a minimum, we hypothesize that this suspended material covaried with phytoplankton biomass.

Microscopic observations reported by Hood et al. [1990] showed that this area 1 week earlier was dominated by the same species assemblage along with an abundance of phytoplankton detritus. Figures 9a and 9b show that there were large changes in fluorescence yield in this regime. Falkowski and Kiefer [1985] have suggested that large changes in fluorescence yield with changes in incident sunlight are typical of rapidly growing populations. Similar patterns were seen in natural populations by Abbott et al. [1982], who also suggested that rapidly growing populations should have a strong fluorescence/light response.

The presence of an upwelling center has been noted in this location southwest of Point Arena (Figure 2) in other years from both ship and satellite observations [Kelly, 1985; Simpson, 1985; Abbott and Zion, 1985]. Given that the winds were only moderate at the time of deployment, it is likely that the upwelling center was weakening. Water velocities at this point as measured by the drifter motion were <20 cm/s, compared with measurements of >50 cm/s in the same location at other times [Davis, 1985a]. The presence of the chain-forming diatom, Chaetocerus, is also consistent with the near-coastal origin of this water. Hood et al. [1990] reported on an extensive survey made during the 10 days prior to the drifter deployment, and they noted that Chaetocerus was constrained to the nearshore portion of their survey grid.

As the drifter moved offshore during days 170–172, the water became significantly different. Temperatures increased (although not smoothly as one might expect if only warming due to solar radiation was occurring), and N+N concentrations decreased to nearly undetectable levels. Both sun-stimulated and strobe-stimulated fluorescence decreased during this period, although there was considerable variability. Water clarity (as indicated by beam attenuation) increased generally, although there was considerable variability in the signal. Much of this variability in clarity was associated with nonfluorescent material, particularly at night. We speculate that the nocturnal variations were largely the result of zooplankton vertically migrating through the transmissometer path, as suggested earlier. The water samples also showed increased abundance of nauplii in this area beginning on day 171. Although neither of these measurements will give an accurate quantitative estimate of zooplankton abundance, they do

suggest that the relative abundance of zooplankton is higher in this region than closer to shore. This result is also consistent with the long-term average derived from the CalCOFI data that shows a zooplankton biomass maximum approximately 100 km offshore [*Chelton*, 1982]. The phytoplankton community has a large component of LCD along with *Rhizosolenia* and *Nitzschia*. The coastal species, *Chaetocerus*, became increasingly rare. LCD also increased during this period, as did the overall cell volume. The fluorescence response of the phytoplankton showed less variation as a function of solar radiation than in the first region, suggesting that the phytoplankton were growing more slowly than nearshore (Figures 9a and 9b).

During this second period, the winds had relaxed and there was evidence of near-surface temperature stratification. There was also considerable high-frequency variability in temperature, presumably a result of increased internal wave activity. Based on the uptake of N+N, phytoplankton were growing rapidly, and there were strong shifts in the species structure of the phytoplankton, particularly of the diatoms. This region is similar to the "typical" upwelling community, which is characterized by diatoms [e.g., *Brink et al.*, 1981; *Estrada*, 1984; *Jones et al.*, 1983]. The sinking rate past the drifter during the second period is estimated to be $w = -(dT/dt)/(\partial T/\partial z)$. With $dT/dt = 1.0°C/day$ and $\partial T/\partial z \approx 0.06°C/m$, then $w \approx -16$ m/day. This sinking rate in the filament is comparable to the upwelling rate along the coast.

The third regime covered days 172 through 174 and was characterized by strong winds on days 172–173. The drifter was moving most rapidly at this point (about 40 cm/s). Temperature increased initially and then leveled off around 13°C, although a strong diurnal cycle was present. N+N concentrations were essentially zero. Water clarity was fairly high with a strong diurnal trend. Transparencies decreased from early morning until near sunset, after which they began to increase until the next morning. This increase was interrupted intermittently, perhaps by vertically migrating zooplankton. During this period, the water sampler caught the highest number of nauplii. The phytoplankton community was dominated by LCD. The fluorescence response of the phytoplankton was less affected by changing light levels than during the second regime.

Despite the strong winds, the nitracline appeared to have been deeper than the mixed layer as there was no apparent increase in near-surface N+N concentrations as might be expected during stronger winds. However, distributions of other properties, notably temperature, strobe-stimulated fluorescence, and beam attenuation showed much less small-scale variability compared to earlier in the deployment. This may have been partially the result of intense mixing, caused by the strong winds during this period (Figure 5a).

Although total cell volumes were nearly 2 orders of magnitude higher in this third period than in the first period, beam attenuation was much lower (roughly 0.73 m^{-1} versus 0.59^{-1}). At first this seems paradoxical, but as was discussed earlier, waters in the first period were probably dominated by small phytoplankton and covarying detrital particles as noted by *Hood et al.* [1990] several days earlier. The *Actinocyclus* species that formed a large component of the LCD group present in the third region is a large cell with little chlorophyll (consistent with the overall decrease in fluorescence and relative increase in downwelling irradiance at 488 nm noted in this region) and a large vacuole. *Hood et al.* [1990] noted that samples from this region were almost exclusively *Actinocyclus* with hardly any debris. Thus cell volume is apparently not an accurate indicator of phytoplankton chlorophyll in this area. Although we do not have independent estimates of phytoplankton carbon, we suspect that they more closely follow the patterns in

beam attenuation and strobe-stimulated fluorescence, rather than cell volume. This assumption is based on the observation that changes in cell volume are largely driven by changes in LCD abundance, which are characterized by a large vacuole.

We cannot calculate chorophyll directly from these data, but if we assume that strobe-stimulated fluorescence is a good indicator of relative chlorophyll content, then this third, offshore region had about one-third the chlorophyll of the first, nearshore region. (Note that the relative change between inshore and offshore chlorophyll extractions discussed earlier are similar to this estimate.) If one uses the formula and parameters proposed by *Bishop* [1986] for the conversion of beam transmission to suspended particulate material (SPM) concentrations, SPM concentrations in the offshore region were approximately one-half those nearshore. Although the reliability of these estimates of biomass is not high (even the extracted chlorophyll estimates may not be representative of the drifter data as the samples were not taken adjacent to the drifter but rather were collected several kilometers away), we note that the general trend is similar for both SPM and estimated chlorophyll with similar magnitude. The lone exception was cell volume, which increased as the drifter moved offshore. If we estimate the relative change in the volume to chlorophyll ratio (based on the cell counts and the relative change in strobe-stimulated fluorescence) between the nearshore region and the offshore region, it is about 300 times larger offshore than nearshore. Results of *Hood et al.* [1990] indicate the cell volume to chlorophyll ratio was about 3 times larger offshore than nearshore. However, the results from *Hood et al.* [1990] are based on Coulter counter volumes and thus include detritus as well as living phytoplankton cells in the estimate of total volume whereas the results here are based on microscopic counts of phytoplankton. If we make the assumption that the estimated SPM concentrations are reasonable indicators of total particulate volume (analogous to the Coulter counter measurements), then the ratio of particulate volume to chlorophyll for the offshore region was about twice that of the nearshore region, similar to the *Hood et al.* [1990] estimates. This suggests that the optical properties of the nearshore region at the upwelling center were significantly affected by the presence of suspended particulates other than phytoplankton and that Coulter counter data from such areas cannot be associated exclusively with phytoplankton. It also shows that changes in chlorophyll content per cell may further complicate interpretation of fluorescence data.

We do not have much confidence in the absolute estimates of SPM from the beam transmissometer since many researchers have shown that there can be considerable variability in the parameters used to estimate SPM from changes in beam attenuation [*Spinrad*, 1986; *Bartz et al.*, 1978; *Bishop*, 1986]. However, the SPM estimates, along with estimates in chlorophyll and total cell volume from phytoplankton counts, do fit into a consistent pattern of change in the composition of suspended particulates as one moves along the core of the filament from its origin to offshore.

This third (offshore) regime appeared to be in balance between phytoplankton growth and zooplankton grazing, particularly on days 173–176 (Figure 7). Beam attenuation shows a strong diurnal cycle, increasing during the day and decreasing (although with considerable high-frequency variation) at night. Strobe-stimulated fluorescence is more difficult to interpret, as changes in fluorescence that may result from changes in chlorophyll content are entangled with changes in fluorescence that result from photoinhibition. However, after allowing for photoinhibition effects, we note that the strobe-stimulated fluorescence decreases at night at about the same time as the beam attenuation data becomes "spiky" (presumably as result of vertical migration of zooplankton). This

decrease in fluorescence continues after sunrise, reaching a minimum around noon, and then recovers in the afternoon until the following midnight. Note that at midnight, beam attenuation and strobe-stimulated fluorescence begin at the same levels for both days 174 and 175. On day 176, the beam attenuation is higher and the strobe-stimulated fluorescence is higher than that on the previous nights. Thus there appears to have been rough equilibrium between the production of organic matter during the day and its subsequent removal at night.

Although we do not have water sampler data to reinforce our position, we suggest that the latter portion of the deployment (days 175 and 176) represented a distinct fourth regime. Total cell volume dropped precipitously in the last sample on day 173, while both fluorescence signals decreased and water transparency increased. Although the winds were calm during this period, there was considerably less small-scale variability in fluorescence and beam attenuation. This regime was probably more typical of an oceanic regime with very low nutrient concentrations, warm temperatures, and a rough balance between phytoplankton growth and removal by zooplankton. Note that on the last day, the drifter appeared to begin to leave this regime and enter an area of increased phytoplankton biomass (as indicated by strobe-stimulated fluorescence) and decreased water transparency. The drifter had changed direction 1 day earlier and was heading toward shore (Figure 2), perhaps resulting in this increase on the last day as the drifter entered more productive nearshore water.

The main goal for the drifter deployment was to estimate the time scales of variability independently of the space scales. However, the processes of subduction, mixing, and entrainment can still confuse spatial variations with temporal variations. In particular, estimates of the sinking of cold water presented earlier suggest that vertical motions are important along the filament. However, for the moment, let us assume that the dominant changes occur in situ; that is, the drifter is moving with a water parcel. If we focus on changes in phytoplankton community composition, we note that the community present in the presumably freshly upwelled water is dominated by *Chaetocerus* spp. and LCD with a high concentration of covarying detrital particles. Within 36 hours, *Chaetocerus* is largely replaced by *Nitzschia* and *Rhizosolenia*, and LCD becomes dominant. One day later, *Nitzschia* is almost absent, and the community now becomes dominated almost exclusively by LCD. Although there is a decrease in the relative abundance of LCD around day 172 (fourth day of deployment), we ascribe this to changes in water masses, rather than biological changes. In summary, we note a shift from a rapidly growing *Chaetocerus/Nitzschia/Rhizosolenia*/LCD community to a more slowly growing LCD community by the end of the water sampler sequence. Given the presence of LCD at the beginning of the deployment at the upwelling center and that the overall increase in total cell volume is largely driven by changes in the abundance of LCD, we suspect that it behaves much like a "seed" population within the filament. After the initial high N+N values are reduced, it appears that the growth of LCD continues for about 2–3 days during which time its growth rate slows substantially. However, during this period the warming of the surface water occurs at a rate such that sinking of cold water must also be occurring. Thus some of the increase in LCD may result from convergence of waters containing LCD.

It appears that much of this apparent "growth" in phytoplankton cell volume is accomplished without any increase in total chlorophyll. That is, as cell volume increases dramatically, chlorophyll as estimated by strobe-stimulated fluorescence actually decreases over time (except on the first day when it increases

after the initial upwelling). Thus the use of cell volume as an indicator of phytoplankton abundance may be somewhat misleading. A more reasonable indicator may be strobe-stimulated fluorescence (after accounting for the diurnal signal in fluorescence yield). If we look at the midnight values, they show an initial increase on the first 2 days, reaching a maximum on day 170. Afterward, they decline steadily, reaching a minimum on day 174 and increasing slightly until the end of the deployment. This pattern is consistent with the general pattern of beam transmission.

While there are several time scales present in all of the various data sets, there does appear to be a dominant scale of 2–3 days for changes in N+N concentration, phytoplankton species composition, total chlorophyll, and fluorescence yield (as an indicator of photosynthetic potential). Similar time scales have been observed in other upwelling systems [e.g., *Ryther et al.*, 1971; *Brink et al.*, 1981; *Jones et al.*, 1983]. However, we caution that our estimates of the time scales may be inaccurate because of slippage, mixing, and exchange with other water masses.

As the Tri-Star drifter does not follow water masses exactly, particularly in areas of large vertical motions, some of our conclusions may not be accurate. We tend to favor the explanation that the filament may be subducting as it moves offshore, leading to change in the optical and biological properties as measured by the fixed-depth drifter. There is strong evidence for subduction from other CTZ data sets (D. Kadko and T. Cowles, personal communication, 1989). Satellite imagery from 1981 of phytoplankton pigment and SST suggest that the offshore end of filaments is characterized by relatively high SST and high pigment off northern California [*Abbott and Zion*, 1985]. As the effective measurement depth of the coastal zone color scanner is larger than the SST measurement (several meters to a few tens of meters versus the upper few microns), this observation is consistent with the scenario that the cold, high pigment water subducts underneath warmer, low pigment water. The net effect is that the satellite sensors "see" the high pigment water at depth and the warm water at the surface. Given the rapid heating of the surface water between days 170 and 173, it appears that the filament was subducting during this period. Decreased N+N concentrations are also consistent with this picture of subduction and subsequent convergence of warmer, more N+N-deficient water.

5. CONCLUSIONS

There is a considerable body of work on the patterns of nutrients, phytoplankton biomass and primary production in upwelling systems. The fundamental picture is that the upwelling center is initially characterized by low phytoplankton biomass, low temperature, and high nutrient values. Rapid growth by phytoplankton reduces the nutrient concentrations as the water warms and moves offshore from the upwelling center. Zooplankton abundance also increases in response to increased food availability. Phytoplankton growth rates then decline, and phytoplankton biomass decreases. Typically, one expects large diatoms present inshore with smaller forms offshore in the low nutrient environment.

Our results do not contradict this basic picture, although they do differ in some of the details. The particular filament that was sampled by the drifter in 1987 was similar to this general picture, although it differed in some respects. For example, the rapidly increasing portion of the phytoplankton population appeared to be large centric diatoms that apparently have a very low chlorophyll:volume ratio. Typically, one expects smaller forms such as chain-forming diatoms (e.g., *Chaetocerus*, *Rhizosolenia*) to dominate such upwelling systems. However, LCD appear to have

an advantage, particularly where nutrient concentrations are decreasing. The role of the large vacuole in LCD in maintaining the position of the population in a high-light environment may be important in such conditions. That is, it may be able to survive low-nutrient periods and then "shift up" [Jones et al., 1983; MacIsaac et al., 1985] rapidly when it enters another area of high nutrients. This particular class of species makes interpretation of cell volume data somewhat difficult, as cell volume may increase although chlorophyll fluorescence may be decreasing.

Nonfluorescent particulates are abundant nearshore, particularly within the upwelling center. These particulates in general covary with fluorescent material. Apparently these particles sink out rapidly as the upwelled water moves offshore. The decrease in their abundance, along with the decrease in phytoplankton abundance (as measured by chlorophyll concentration), is largely responsible for the overall increase in water transparency. Total cell volume increases, though, largely because of the increase in LCD abundance. Short-term changes in transparency, especially after sunset, appear to be caused by zooplankton. Diurnal changes apparently result from phytoplankton growth during the day and zooplankton grazing (or sinking of phytoplankton) at night. As expected, photosynthetic (as indicated by fluorescence response) rates are highest nearshore and decrease as the upwelled water moves offshore. This decrease moves in parallel with the decrease in N+N. Populations offshore are still viable although apparently any biomass accumulation during the day is balanced by losses at night.

The "aging" of the upwelled water, as manifested in changes in phytoplankton biomass, species composition, primary productivity, nutrient levels, temperature, and water transparency, occurs rapidly. Large changes in these variables can take place in 2–3 days. Given that the dominant scales of wind forcing and surface currents in this area are about 4–5 days [Kosro, 1987; Winant et al., 1987], we note that there is a close correspondence between the scales of biological variability and physical forcing. The consequent coupling is probably important in maintaining the high productivity of upwelling ecosystems.

One model for the filaments suggests that they are the result of the interaction of a meandering southward current (in this case, the California Current) with cold, nutrient-rich upwelled water near the coast. Because of variations in alongshore wind stress and coastal topography, upwelling occurs in distinct "centers," and this alongshore variation may lead to local intensification of the seaward moving portion of the meander [e.g., Davis, 1985b]. This intensification may be the cold filament readily observed in satellite images [Coastal Transition Zone Group, 1988]. If such a model is correct, then one might expect phytoplankton species that are present at the northern end of the meandering current to be advected southward, alternately being nearshore in nutrient-replete conditions, and then being offshore in nutrient-deficient conditions. Certainly, there will be departures from such a simple model as we expect there to be significant exchange between the meander waters and the surrounding oceanic and coastal waters. Given typical near-surface water velocities, we expect that a complete circuit from one center to another along a meander will be of the order of 10 days. Such conditions might favor species that react rapidly to changes in the nutrient regime and yet remain viable in the upper ocean during nutrient-deficient periods. When such species encounter high nutrients, they will be able to grow rapidly as they will be adapted for high light. Perhaps LCD with its large vacuole and high volume to chlorophyll ratio might be representative of such a set of species. Although the data are not available to study this question, one

could examine the distribution of LCD along the length of the California Current in relation to the upwelling centers. If such a model were correct, one would expect to find a fairly stable "pool" of LCD with maximum values being located seaward of the upwelling centers along the meanders. This picture differs from that presented by Jones et al. [1988] for the Point Conception upwelling system. Their model was of an asymmetric upwelling center with low phytoplankton, high nutrient concentrations on the poleward side of an upwelling center and high chlorophyll, high nutrient concentrations on the equatorward side. Our results suggest that much of this "asymmetry" may result from rapid temporal changes along the filament rather than spatial changes. However, it is likely that the dynamics of upwelling off Point Conception, where the coastline is highly irregular, are different than those off northern California.

This present data set is not sufficient to make conclusive statements concerning exchange rates between the cold filament and the surrounding waters. Slippage of the drifter cannot be easily be mistaken for mixing, but since we lack detailed information on the properties of the surrounding water, slippage can be a problem. Bucklin et al. [1989] show that particle advection in the geostrophic flow in a filament is not affected by more than a few kilometers with the expected small-scale horizontal diffusivities. However, the phytoplankton species information can be used to indicate the relative importance of exchange and in situ processes for the period when water samples were available (days 168–173). The nearshore upwelling center is initially dominated by chain-forming diatoms and LCD. As the water advects offshore, the phytoplankton rapidly becomes dominated by LCD. We suggest that this change in phytoplankton composition between days 168 and 173 is largely an in situ process, as LCD is generally found only within filaments rather than in the surrounding waters [Hood et al., 1990]. That is, the increase in LCD was a result of growth of the initial population, rather than mixing and exchange although convergence probably plays some role in this increase.

Future experiments using clusters of similarly equipped drifters will help unravel temporal variations from spatial variations. We also should be able to estimate Lagrangian decorrelation time scales with such clusters of instrumented drifters. However, we also note that the availability of water samples concurrent with more automated optical sensors is essential at this early stage in research with Lagrangian drifters. We need to gain considerably more experience with such comparisons between optical instruments and traditional sampling techniques in order to interpret the optical data properly.

REFERENCES

Abbott, M. R., P. J. Richerson, and T. M. Powell, In situ response of phytoplankton fluorescence to rapid variations in light, *Limnol. Oceanogr., 27,* 218–225, 1982.

Abbott, M. R., and P. M. Zion, Satellite observations of phytoplankton variability during an upwelling event, *Cont. Shelf. Res., 4,* 661–680, 1985.

Abbott, M. R., and P. M. Zion, Spatial and temporal variability of phytoplankton pigment off northern California during Coastal Ocean Dynamics Experiment 1, *J. Geophys. Res., 92,* 1745–1755, 1987.

Bartz, R., R. V. Zaneveld, and H. Pak, A transmissometer for profiling

and moored observations in water, *Proc. Soc. Photo. Opt. Eng.*, *160*, 102–108, 1978.

Beers, J. R., M. R. Stevenson, R. W. Eppley, and E. R. Brooks, Plankton populations and upwelling off the coast of Peru, June 1969, *Fish. Bull.*, *69*, 859–876, 1971.

Bishop, J. K. B., The correction and suspended material calibration of Sea Tech transmissometer data, *Deep Sea Res.*, *33*, 121–134, 1986.

Booth, C. R., and R. C. Smith, Moorable spectroradiometers in the Biowatt experiment, *Proc. Soc. Photo. Opt. Eng.*, *925*, 176–188, 1988.

Booth, C. R., B. G. Mitchell, and O. Holm-Hansen, Development of moored oceanographic spectroradiometer, Biospherical *Tech. Rep.*, *87-1*, Biospherical Instrum. Inc., San Diego, Calif., 1987.

Breaker, L. C., and R. P. Gilliland, A satellite sequence on upwelling along the California coast, in *Coastal Upwelling*, Coastal and Estuarine Sci., vol. 1, edited by F. A. Richards, pp. 87–94, AGU, Washington, D.C., 1981.

Brink, K. H., B. H. Jones, J. C. Van Leer, C. N. K. Mooers, D. W. Stuart, M. R. Stevenson, R. C. Dugdale, and G .W. Hebum, Physical and biological structure and variability in an upwelling center off Peru near 15°S during March 1977, in *Coastal Upwelling*, Coastal and Estuarine Sci., vol. 1, edited by F. A. Richards, pp. 473–495, AGU, Washington, D.C., 1981.

Bucklin, A., M. M. Rienecker, and C. N. K. Mooers, Genetic tracers of zooplankton transport in coastal filaments off northern California, *J. Geophys. Res.*, *94*, 8277–8288, 1989.

Chelton, D. B., Large-scale response of the California Current to forcing by wind stress curl, *CalCOFI Rep.* 23, pp. 130–148, Calif. Coop. Fish. Invest., La Jolla, 1982.

Coastal Transition Zone Group, The Coastal Transition Zone program, *Eos Trans. AGU*, *69*, 698–699, 1988.

Davis, R. E., Drifter observations of coastal surface currents during Coastal Ocean Dynamics Experiment: The method and descriptive view, *J. Geophys. Res.*, *90*, 4741–4755, 1985a.

Davis, R. E., Drifter observations of coastal surface currents during Coastal Ocean Dynamics Experiment: The statistical and dynamical views, *J. Geophys. Res.*, *90*, 4756–4772, 1985b.

Dickey, T. D., Recent advances and future directions in multi-disciplinary in situ oceanographic measurement systems, in *Toward a Theory on Biological-Physical Interactions in the World Ocean*, edited by B. J. Rothschild, pp. 555–598, Kluwers, Dordrecht, The Netherlands, 1988.

Dickey, T. D., E. Hartwig, and J. Marra, The Biowatt bio-optical and physical moored measurement program, *Eos Trans. AGU*, *67*, 650–651, 1986.

Estrada, M., Phytoplankton distribution and composition off the coast of Galicia (northwest Spain), *J. Plankton Res.*, *6*, 417–434, 1984.

Falkowski, P., and D. A. Kiefer, Chlorophyll *a* fluorescence in phytoplankton: Relationship to photosynthesis and biomass, *J. Plankton Res.*, *7*, 715–731, 1985.

Flament, P., L. Armi, and L. Washburn, The evolving structure of an upwelling filament, *J. Geophys. Res.*, *90*, 11,765–11,778, 1985.

Friederich, G. E., P. J. Kelly, and L. A. Codispoti, An inexpensive moored water sampler for investigating chemical variability, in *Tidal Mixing and Plankton Dynamics*, edited by M. J. Bowman, C. M. Yentsch, and W. T. Peterson, pp. 463–482, Springer-Verlag, New York, 1986.

Fukuchi, M., H. Hattori, H. Sasaki, and T. Hoshiai, A phytoplankton bloom and associated processes observed with a long-term moored system in Antarctic water, *Mar. Ecol.*, *45*, 279–288, 1988.

Gordon, H. R., O. B. Brown, R. H. Evans, J. W. Brown, R. C. Smith, K. S. Baker, and D. K. Clark, A semianalytic radiance model of ocean color, *J. Geophys. Res.*, *93*, 10,909–10,924, 1988.

Harris, G. P., The relationship between chlorophyll *a* fluorescence, diffuse attenuation changes and photosynthesis in natural phytoplankton populations, *J. Plankton Res.*, *2*, 109–128, 1980.

Hood, R., M. R. Abbott, P. M. Kosro, and A. Huyer, Relationships between physical structure and biological pattern in the surface layer of a northern California upwelling system, *J. Geophys. Res.*, in press, 1990.

Ikeda, M., and W. J. Emery, Satellite observations and modeling of meanders in the California Current System off Oregon and northern California, *J. Phys. Oceanogr.*, *14*, 1434–1450, 1984.

Jones, B. H., K. H. Brink, R. C. Dugdale, D. W. Stuart, J. C. Van Leer, D. Blasco, and J. C. Kelley, Observations of a persistent upwelling center off Point Conception, California, in *Coastal Upwelling: Its Sediment Record. Responses of the Sedimentary Regime to Present Coastal Upwelling*, edited by E. Suess and J. Thiede, pp. 37–60, Plenum, New York, 1983.

Jones, B. H., L. P. Atkinson, D. Blasco, K. H. Brink, and S. L. Smith, The asymmetric distribution of chlorophyll associated with a coastal upwelling center, *Cont. Shelf Res.*, *8*, 1155–1170, 1988.

Kelly, K. A., The influence of winds and topography on the sea surface temperature patterns over the northern California slope, *J. Geophys. Res.*, *90*, 11,783–11,798, 1985.

Kiefer, D. A., Fluorescence properties of natural phytoplankton populations, *Mar. Biol.*, *22*, 263–269, 1973.

Kosro, P. M., Structure of the coastal current field off northern California during the Coastal Ocean Dynamics Experiment, *J. Geophys. Res.*, *92*, 1637–1654, 1987.

Kosro, P. M., and A. Huyer, CTD and velocity surveys of seaward jets off northern California, July 1981 and 1982, *J. Geophys. Res.*, *91*, 7680–7690, 1986.

MacIsaac, J. J., R. C. Dugdale, R. T. Barber, D. Blasco, and T. T. Packard, Primary production cycle in an upwelling center, *Deep Sea Res.*, *32*, 503–529, 1985.

Mackas, D. L., W. R. Crawford, and P. P. Niiler, A performance comparison for two Lagrangian drifter designs, *Atmos. Ocean*, *27*, 443–456, 1989.

Mooers, C. N. K., and A. R. Robinson, Turbulent jets and eddies in the California Current and inferred cross-shore transports, *Science*, *223*, 51–53, 1984.

Niiler, P. P., R. E. Davis, and H. J. White, Water-following characteristics of a mixed layer drifter, *Deep Sea Res.*, *34*, 1867–1881, 1988.

Poulain, P. M., J. D. Illeman, and P. P. Niiler, Drifter observations in the California Current system, *Ref. 87-27*, 72 pp., Scripps Inst. of Oceanogr., Univ. of Calif., San Diego, La Jolla, 1987.

Ryther, J. H., D. W. Menzel, E. M. Hulburt, C. J. Lorenzen, and N. Corwin, Production and utilization of organic matter in the Peru coastal current, *Anton Bruun Rep. 4.*, Tex. A and M Univ., College Station, 1971.

Scripps Institution of Oceanography, Physical, chemical, and biological data, CLIMAX I cruise, *Ref. 74-20*, 40 pp., Univ. of Calif., San Diego, La Jolla, 1974.

Scripps Institution of Oceanography, Physical, chemical, and biological data, CalCOFI cruise 8404, CalCOFI cruise 8405, CalCOFI cruise 8406, *Ref. 84-25*, 224 pp., Univ. of Calif., San Diego, La Jolla, 1984.

Siegel, D. A., T. D. Dickey, L. Washburn, M. K. Hamilton, and B. G. Mitchell, Optical determination of particle abundance and production variations in the oligotrophic ocean, *Deep Sea Res.*, *36*, 211–222, 1989.

Simon, R. L., The summertime stratus over the offshore waters of California, *Mon. Weather Rev.*, *105*, 1310–1314, 1977.

Simpson, J. J., Air-sea exchange of carbon dioxide and oxygen induced by phytoplankton: Methods and interpretation, in *Mapping Strategies in Chemical Oceanography*, edited by A. Zirino, pp. 409–450, American Chemical Society, Washington, D.C., 1985.

Smith, R. C., C. R. Booth, and J. L. Star, Oceanographic bio-optical profiling system, *Appl. Opt.*, *23*, 2791–2797, 1984.

Spinrad, R. W., A calibration diagram of specific beam attenuation, *J. Geophys. Res.*, *91*, 7761–7764, 1986.

Traganza, E. D., V. M. Silva, D. M. Austin, W. L. Hanson, and S. H. Bronsink, Nutrient mapping and recurrence of coastal upwelling centers by remote sensing: Its implication to primary production and the sediment record, in *Coastal Upwelling: Its Sediment Record. Responses of the Sedimentary Regime to Present Coastal Upwelling*, edited by E. Suess and J. Thiede, pp. 61–83, Plenum, New York, 1983.

Tyler, J. E., R. W. Austin, and T. J. Petzold, Beam transmissometer for oceanographic measurements, in *Suspended Solids in Water*, edited by J. R. Gibbs, pp. 51–60, Plenum, New York, 1974.

Walsh, J. J., C. D. Wirick, L. J. Pietrafesa, T. E. Whitledge, F. E. Hoge, and R. N. Swift, High-frequency sampling of the 1984 spring bloom within the Mid-Atlantic Bight: synoptic shipboard, aircraft, and in situ perspectives of the SEEP-1 experiment, *Cont. Shelf Res.*, *8*, 529–563, 1988.

Whitledge, T. E., and C. D. Wirick, Observations of chlorophyll concentrations off Long Island from a moored in situ fluorometer, *Deep Sea Res.*, *30*, 297–309, 1983.

Willmott, A. J., Forced double Kelvin waves in a stratified ocean, *J. Mar. Res.*, *42*, 319–358, 1984.

Winant, C. D., R. C. Beardsley, and R. E. Davis, Moored wind, temperature, and current observations made during Coastal Ocean Dynamics Experiments 1 and 2 over the northern California continental shelf and upper slope, *J. Geophys. Res.*, *92*, 1569–1604, 1987.

M. R. Abbott, College of Oceanography, Oregon State University, Corvallis, OR 97331.

K. H. Brink, Woods Hole Oceanographic Institution, Woods Hole, MA 02543.

C. R. Booth, Biospherical Instruments, Inc., 4901 Morena Boulevard, San Diego, CA 92110.

D. Blasco, Bigelow Laboratory for Ocean Sciences, McKown Point, West Boothbay Harbor, ME 04575.

L. A. Codispoti, Monterey Bay Aquarium Research Institute, 160 Central Avenue, Pacific Grove, CA 93950

P. P. Niiler, Scripps Institution of Oceanography, University of California, San Diego, La Jolla, CA 92093

S. R. Ramp, Department of Oceanography, U.S. Naval Postgraduate School, Monterey, CA 93943